

Design of an IoT-Based Automatic Switching and Monitoring System for Hybrid Power Plants

Anggi Aguska^{1*}, Subuh Isnur Haryudo¹, Unit Three Kartini¹, Miftahur Rohman¹

¹Department of Electrical Engineering, Faculty of Engineering, State University of Surabaya
Jl. Ketintang, Ketintang, Gayungan, Surabaya City, East Java, Indonesia-60231

*Corresponding author: anggiaguska.20052@mhs.unesa.ac.id Doi: <https://doi.org/10.24036/invotek.v24i1.1179>

This work is licensed under a Creative Commons Attribution 4.0 International License



Abstract

Hybrid power generation, a power plant that combines two or more plants, continues to grow along with technological advances. The performance of these power plants relies heavily on effective switching and monitoring systems. Monitoring data is critical in maintenance scheduling, preventive intervention, and the timely identification and assessment of environmental changes. One of the switching and monitoring technologies integrated with the Internet is the Internet of Things (IoT) technology. This study introduces a system design capable of wirelessly performing switching operations and transmitting real-time data to a hybrid power plant monitoring system through an application. Test results demonstrate that the system successfully executes automatic switching between the hybrid power plant and the PLN electricity grid based on accumulator voltage thresholds. The monitoring data analysis reveals MAPE values of 2.959% and 3.577% for the voltage and current of the hybrid power plant, and a MAPE of 1% for the accumulator voltage. The voltage and load current readings also exhibit MAPEs of 0.604% and 8.625%. Based on the test results, it can be concluded that this device shows the ability of the system to automate the switching of resources to the load and monitor the hybrid power plant very well, with the smallest MAPE value achieved of 0.604%.

Keywords: Switching System, Monitoring System, Hybrid Power Plant, Internet of Things.

1. Introduction

The rise in electricity tariff (ET) is increasing the demand for electrical energy due to national electricity company (PLN) continued reliance on fossil fuel-based sources [1]. This reliance poses a significant threat to future energy sustainability as fossil fuel reserves are depleting [2]. Indonesia primarily relies on coal-fired power plants (CFPP) and the country's current coal reserves stand at 38.84 billion tonnes, with an annual production rate of 600 million tonnes expected to last approximately 65 years without additional reserves [3]. However, uncontrolled coal usage would accelerate the depletion of these reserves and worsen environmental pollution by emitting harmful pollutants such as sulfur oxides (SO_x), nitrogen oxides (NO_x), carbon monoxide (CO), and fly ash [4].

Positioned along the equator, Indonesia enjoys abundant solar irradiance, with an estimated potential of 4.5 kW/m²/day, making solar energy a viable component of the nation's renewable energy portfolio [5]. Under these auspicious circumstances, Indonesia stands poised to leverage solar energy as a prominent facet of its burgeoning new and renewable energy (NRE) sector. In recent times, there has been discernible momentum in the advancement of solar power as a viable alternative energy source within the Indonesian landscape [6]. Solar energy is free and abundant compared to other energy sources [7].

Monitoring systems are crucial for ensuring the effectiveness and performance of photovoltaic (PV) systems. These systems play a pivotal role in data collection and transmission to the control center, assisting users in comprehensive assessment, evaluation, and management of the system. The purpose is to mitigate maintenance costs, monitor operational performance, and promptly identify faults within the PV system [8], [9]. Monitoring proves indispensable due to the dynamic nature of solar radiation

levels, which fluctuate in response to geographical location, diurnal variations, and prevailing climatic conditions [10]. The entirety of monitoring data serves as a valuable reference for maintenance scheduling, preemptive interventions, and timely identification and assessment of environmental alterations. Among the real-time monitoring methodologies employed, Internet of Things (IoT) technology emerges as a salient approach [11].

Research on photovoltaic monitoring systems has been conducted by several researchers [12], [13]. Sutikno et al. [12] designed a system to monitor key parameters, including solar radiation, ambient temperature, voltage, current, and PV output power. This system utilized a combination of photodiodes, DHT22 sensors, voltage sensors, and ACS712 sensors. The NodeMCU V3 ESP8266 served as the primary controller and WiFi gateway, facilitating wireless data transmission to both a monitoring web interface and the Thingspeak platform, obviating the need for an external WiFi module. Research conducted by Readyansyah et al. [13] designed a hybrid power plant that integrates solar cells and thermoelectric generators (TEG), combining Internet of Things (IoT)-based monitoring. This system monitors PV voltage, current, and output parameters using INA219 and PZEM-004T sensors. Arduino Uno serves as the primary controller, while NodeMCU V3 ESP8266 functions as the WiFi gateway, facilitating wireless data transmission to the Blynk platform. Further research was undertaken by Pamungkas et al. [14], focusing on the development of an Internet of Things (IoT)-based photovoltaic power monitoring system. This system meticulously monitors PV output voltage, current parameters, and solar radiation levels utilizing ACS712 sensors, voltage sensors, and BH 1750 sensors. The Arduino Uno is designated as the principal controller, complemented by the NodeMCU V3 ESP8266 acting as the WiFi gateway, facilitating wireless data transmission to the Blynk application. In a study conducted by Inayah et al. [15] INA219 sensors were employed to ascertain the voltage and current parameters produced by solar panels, while DHT22 sensors were utilized to gauge the temperature attributes of solar panels. The ESP32 microcontroller was tasked with processing inputs comprising sensor readings derived from solar panels, subsequently transmitting the computed values to the Blynk platform.

Despite these advancements, PV cells convert only 10% to 20% of incoming solar radiation into electricity, with the rest dissipating as heat [16]. High temperatures negatively impact PV system performance, underscoring the need for hybrid models like PV and thermoelectric generators to meet Indonesia's growing electricity demand sustainably [17]. Embracing hybrid power generation models, such as the integration of photovoltaic and thermoelectric generator (TEG) systems, presents an environmentally conscious approach to meeting the burgeoning electricity demand in Indonesia.

Based on the relevant background and previous research, the researchers are interested in designing an IoT-based hybrid power plant monitoring system that combines photovoltaic and thermoelectric generators with new innovations in accumulator voltage monitoring and monitoring graphic displays using the Firebase Database and Kodular platform and switching power sources to loads locally and remotely with a manual or automatic mode based on the accumulator voltage value. The purpose of this research is to implement an automatic switching system in a hybrid power plant that can automatically connect to the PLN power grid when the battery capacity decreases and monitor the voltage and current of the hybrid power plant, the voltage of the accumulator, the voltage and current of the load in an IoT-based application. The system is expected to deliver good performance, enhancing the quality of maintenance scheduling and preventive interventions, while also preventing excessive accumulator draining to prolong the accumulator's service life.

2. Methodology

In this study, the experimental method will serve as the primary approach, facilitating data collection through both manual testing of electrical energy source switching via selector switches or IoT applications and automated switching based on accumulator voltage. Figure 1 is the research flow used. First, a literature study is a stage carried out to search, read, and evaluate various sources of information related to the topic or problem to be discussed in a study. The second stage is to design the system as a whole to get the expected way the device works. This design includes the selection of the necessary components, the connection between components, and the application design. The third stage is collecting materials to prepare materials that will be designed at the tool design implementation stage. The fourth stage designs the tool to describe in detail the wiring used in the system design. Furthermore, the fifth stage of implementation is where the monitoring and switching system design is made or

realized in the form of a tool based on system design and tool design. The sixth stage of tool testing is carried out to ensure the performance of the tool functions properly accordingly. Seventh, data analysis is a critical stage in the research or information-gathering process, where data has been obtained from the work of the device. The last stage, the conclusion is a summary of the results of the research process.

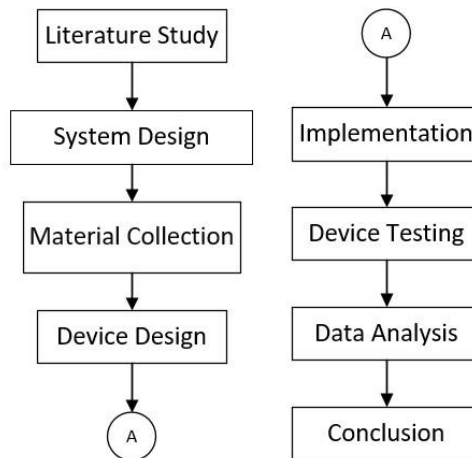


Figure 1. Research Flow

2.1 System Design

The system proposed in this study serves the purpose of enabling automatic switching between electricity sources from hybrid power plants or PLN power sources to loads, alongside the concurrent monitoring of voltage and current parameters about hybrid power plants, accumulator voltage, as well as voltage and current readings of loads, all facilitated through IoT applications. A system design delineating the architecture of the automatic switching system and monitoring mechanism for the IoT-based hybrid power plant is presented in Figure 2.

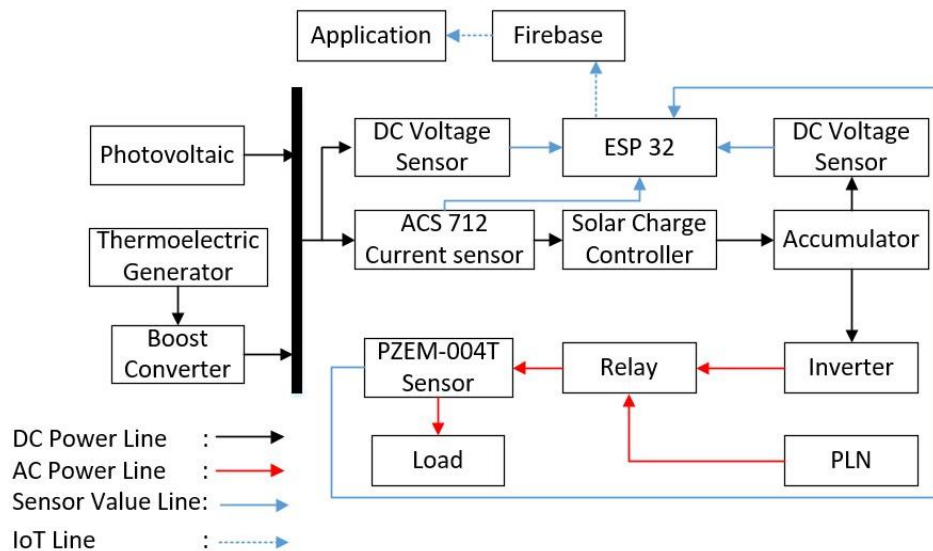


Figure 2. System Design

The hybrid power plant integrates two distinct power generation systems, namely photovoltaic (PV) and thermoelectric generator (TEG), which are synergistically combined to optimize energy output. Voltage and current readings from the hybrid power plant are obtained through the utilization of a DC voltage sensor and an ACS712 current sensor. Subsequently, the generated electrical output is directed to a solar charge controller for accumulator charging, with the accumulator voltage monitored by the DC voltage sensor. Conversion of stored DC energy to AC is facilitated by an inverter. An autonomous switching mechanism, driven by accumulator voltage levels or manually via a local selector switch or IoT application, selects the power source for use. The chosen power source is then supplied to

a load, represented by a 45-watt lamp. Voltage and current measurements of the load are captured by a PZEM-004T sensor. All sensor data is relayed to an ESP32 microcontroller for processing and subsequent transmission to the Firebase Database depicted in Figure 3. This database serves as a repository for sensor readings from the ESP32 and facilitates bidirectional communication by storing switching commands from the application and relaying them to the ESP32.

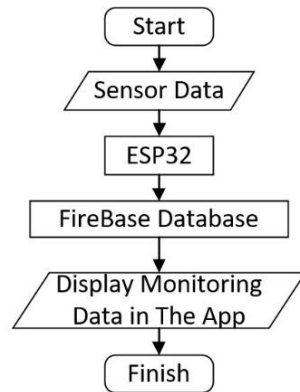


Figure 3. Monitoring Workflow

Figure 4 shows the workflow of the developed hybrid power plant switching system. When the control selector switch is set to the local position, the local selector switch operates, while the remote switch remains inoperative. Conversely, when the control selector switch is set to the remote position, the remote selector switch becomes operational while the local selector switch is inoperative. Furthermore, two operational modes are available in the remote control condition: manual and automatic. In manual mode, the source switch is used to control the position of the power source, while in automatic mode, the switching of the power source is regulated based on the accumulator voltage value. Automatic switching occurs based on predefined thresholds: when the accumulator voltage equals or exceeds 14.9 volts, the system initiates automatic electricity source switching from the hybrid power plant to the PLN electricity source. Conversely, when the accumulator voltage falls below or equals 11.75 volts, automatic power source switching from the hybrid power plant to the PLN power source is triggered.

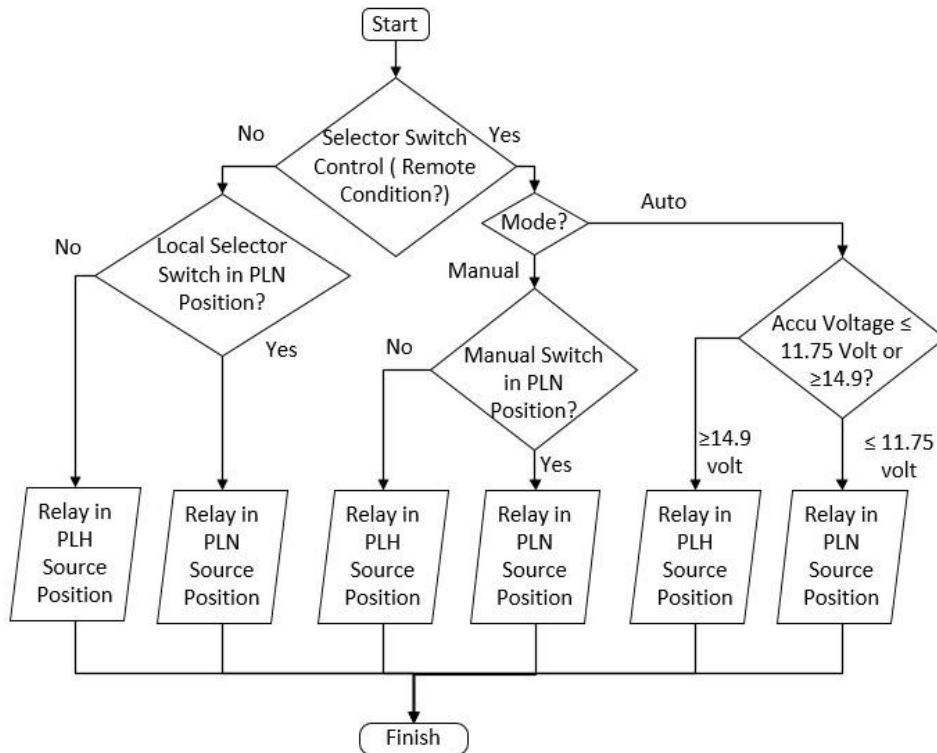


Figure 4. Switching Workflow

2.2 Device Design

The device design of the automatic switching system and monitoring of the IoT-based hybrid power plant are illustrated in Figure 5. The solar panel charges the battery through a solar charge controller. The system includes several sensors and relays to manage and monitor the current and voltage of the plant. The ESP32 microcontroller coordinates the components and sends sensor reading data to Firebase which is then displayed on the app. Local control is provided by two selector switches. The relays control the connection to the inverter and the power grid (PLN), ensuring a continuous supply of power to the load, represented by the lights.

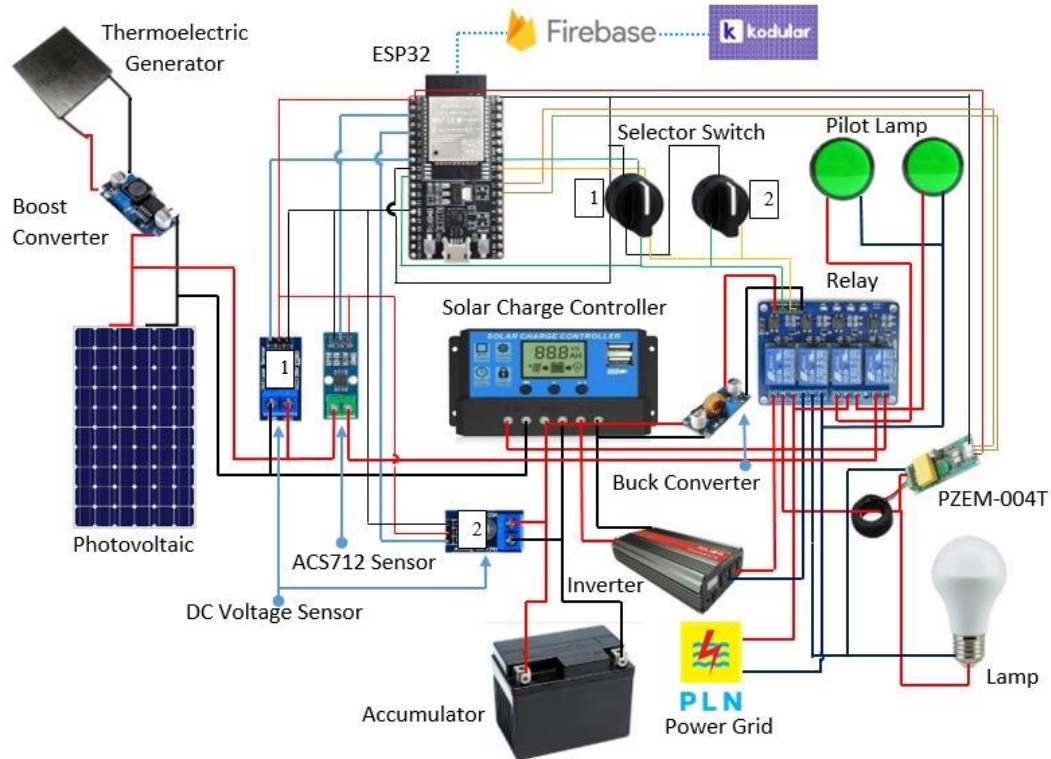


Figure 5. Device Design

In the device design, there are pins used to connect each component. These pins have an important role in ensuring the alignment and continuity of the overall device function. Each pin to be used will be programmed on the ESP32 to match its function. Table 1 shows the pins used in the wiring mentioned earlier.

Table 1. Device Design Pin Configuration

| No. | Component | ESP32 Pin | Connected to |
|-----|------------------------|-----------|--------------|
| 1. | Relay Module 4 Channel | 5V | VCC |
| | | 19 | IN1 |
| | | 19 | IN2 |
| | | 18 | IN3 |
| | | 18 | IN4 |
| | | GND | GND |
| 2. | ACS712 Sensor | 5V | VCC |
| | | VN | OUT |
| | | GND | GND |
| 3. | DC Voltage Sensor 1 | 3V3 | VCC |
| | | 33 | S |
| | | GND | GND |

| No. | Component | ESP32 Pin | Connected to |
|-----|---------------------|-----------|--------------|
| 4. | DC Voltage Sensor 2 | 3V3 | VCC |
| | | 34 | S |
| | | GND | GND |
| 5. | PZEM-004T Sensor | 5V | VCC |
| | | 17 | RX |
| | | 16 | TX |
| | | GND | GND |
| 6. | Selector Switch 1 | GND | NO |
| | | 18 | NC |
| | | 19 | NC |
| 7. | Selector Switch 2 | 18 | NC |
| | | 19 | NO |

3. Result and Discussion

3.1 Device Design Results

3.1.1 Hybrid Power Plant Automatic Switching and Monitoring System Device

Figure 6a depicts the outcomes of the automatic switching system and monitoring design for IoT-based hybrid power plants. The device comprises three primary components: the initial panel box housing the hybrid power plant switching and monitoring circuit, which features essential elements such as the selector switch, pilot lamp indicator, ESP32 microcontroller, 4-channel relay module, DC voltage sensor, ACS712 current sensor, PZEM-004T sensor, buck converter, and boost converter. The second segment encompasses the photovoltaic installation, inclusive of the solar charge controller, inverter, accumulator, and power outlet components. The final section comprises the load circuit, incorporating power cables, light fittings, and lamps. Figure 6b presents an illustration of a hybrid power plant integrating photovoltaic and thermoelectric generator technologies.

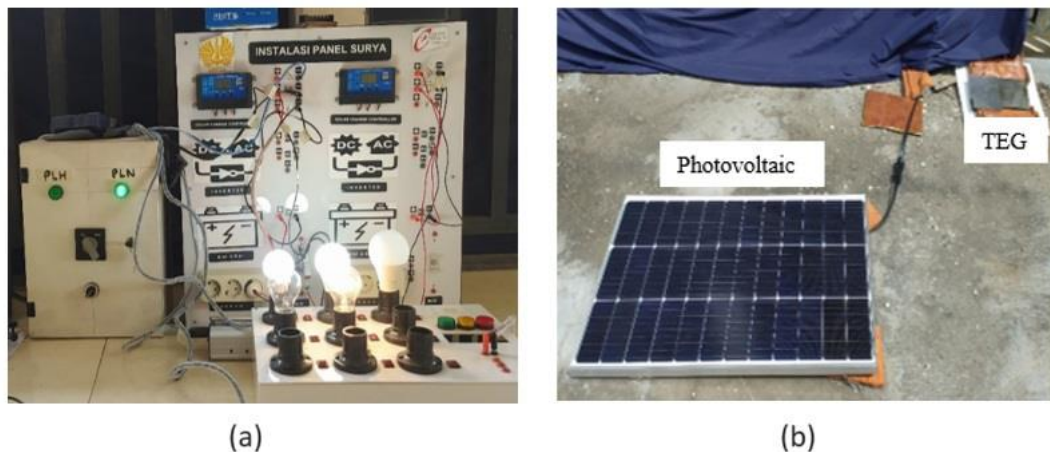


Figure 6. a. Design Results of an Automatic Switching and Monitoring System, b. Hybrid Photovoltaic Power Plant with Thermoelectric Generator (TEG)

3.1.2 IoT Applications

Figure 7a depicts the primary interface of the IoT application utilized for switching and monitoring hybrid power plants. The main page features three distinct menus: monitoring, switching, and graphics. Figure 7b showcases the monitoring menu page, exhibiting indicators of voltage, current, power output of the hybrid power plant, voltage level, and percentage of the accumulator, as well as voltage, current, and power at the load. Figure 7c illustrates the switching menu page, which provides indicators of the electricity source in use, the selected switching mode, the position of the control switch,

and the voltage value and percentage of the accumulator. Figure 7d displays the monitoring graph page, where monitoring data is visualized in the form of a line graph.



Figure 7. a. IoT Application Main Page, b. Hybrid Power Plant Monitoring Menu, c. Hybrid Power Plant Switching Menu, d. Hybrid Power Plant Monitoring Graph Menu

3.2 DC Voltage Sensor and ACS712 Current Sensor Testing on Hybrid Power Plant

Testing procedures entail the examination of voltage and current values derived from the hybrid generator within the monitoring application. Voltage readings are obtained through the DC voltage sensor, while current readings are acquired via the ACS712 current sensor. DC Voltage sensors are designed to measure the amount of direct current electrical voltage in a system or electronic component. This module operates on the principle of a resistive voltage divider, which allows it to accept an input voltage of 5 V or 3.3 V with a DC voltage reading range of 0-25 VDC. ACS712 is a current sensor with a Hall Effect principle that can read AC or DC accurately at an affordable price [18]. This sensor can read currents in the 5A range. Analytical of monitoring values involves error calculation using the absolute percentage error (APE) formula. The calculation formula can be written in Equation (1). The error value data that has been calculated using equation (1), can then be used to find the mean absolute percentage error (MAPE) value which is written in equation (2). The value of equation (2) is used as the average error value obtained from the amount of data from APE compared to the amount of existing data.

$$APE = \text{abs} \frac{\text{Monitoring Value} - \text{Multimeter Value}}{\text{Multimeter Value}} \times 100 \% \quad (1)$$

$$MAPE = \frac{\sum APE}{\text{total data}} \times 100 \% \quad (2)$$

In Equation (1), it is pertinent to note that all calculated values are considered positive absolute values. Table 2 presents a comparison of voltage and current readings from a multimeter and a monitoring system using a DC voltage sensor and ACS712 current sensor, covering various time points throughout the day. The voltage readings from both instruments are generally close, although discrepancies are notable at 10:00 and 12:00, with the error percentage for voltage ranging from 0.247% to 4.394%. Current readings show more variation, particularly in the morning, with error percentages ranging from 0.000% to 6.419%. The mean absolute percentage error (MAPE) is 2.959% for voltage and 3.577% for current. Notably, the power source alternates between PLN and PLH, with a transition to PLH around 14:00 showing consistent voltage monitoring and zero current readings as expected due to the avoidance of simultaneous drain and charge processes. Noise interference in the sensor output signal may contribute to discrepancies in reading values, originating from diverse sources such as electromagnetic disturbances or internal noise inherent to the sensor itself [19], [20]. Moreover, the sensor's reliance on a reference voltage for measurement poses another potential source of error instability or inadequacy in the reference voltage, which can exert influence on sensor readings. The monitoring system generally performs within acceptable limits, though calibration may be needed to reduce current measurement discrepancies.

Table 2. DC Voltage Sensor and ACS712 Current Sensor Testing Results on Hybrid Power Plant

| Time | Multimeter | | Monitoring | | Error Percentage (%) | | Power Source Position |
|-------|----------------|------------------|----------------|------------------|----------------------|---------|-----------------------|
| | Voltage (Volt) | Current (Ampere) | Voltage (Volt) | Current (Ampere) | Voltage | Current | |
| 09.00 | 14.35 | 2.80 | 13.93 | 2.82 | 2.927 | 0.714 | PLN |
| 09.30 | 14.77 | 2.93 | 14.18 | 2.77 | 3.995 | 5.461 | PLN |
| 10.00 | 14.88 | 3.10 | 14.3 | 2.98 | 3.898 | 3.871 | PLN |
| 10.30 | 15.08 | 3.16 | 14.33 | 3.09 | 4.973 | 2.215 | PLN |
| 11.00 | 15.31 | 4.15 | 14.47 | 4.41 | 5.487 | 6.291 | PLN |
| 11.30 | 15.02 | 3.20 | 14.36 | 3.04 | 4.394 | 5.000 | PLN |
| 12.00 | 15.10 | 3.13 | 14.44 | 3.17 | 4.371 | 1.278 | PLN |
| 12.30 | 15.12 | 3.08 | 14.68 | 2.97 | 2.910 | 3.571 | PLN |
| 13.00 | 15.05 | 2.93 | 14.55 | 2.91 | 3.322 | 0.683 | PLN |
| 13.30 | 15.20 | 2.84 | 14.72 | 2.65 | 3.158 | 6.690 | PLN |
| 14.00 | 22.00 | 0.00 | 22.28 | 0.00 | 1.273 | 0.00 | PLH |
| 14.30 | 22.19 | 0.00 | 22.32 | 0.00 | 0.586 | 0.00 | PLH |
| 15.00 | 22.11 | 0.00 | 22.44 | 0.00 | 1.493 | 0.00 | PLH |
| 15.30 | 21.98 | 0.00 | 22.19 | 0.00 | 0.955 | 0.00 | PLH |
| 16.00 | 21.76 | 0.00 | 21.9 | 0.00 | 0.643 | 0.00 | PLH |
| MAPE | | | | | 2.959 | 3.577 | |

Description: PLH: Source of Electricity from Hybrid Power Plant

PLN: Source of Electricity from PLN Electricity Network

3.3 Automatic Switching Testing

The testing protocol involves adjusting the voltage output of the DC power supply to simulate accumulator voltage conditions, ranging from 11.75 volts to 15 volts. The voltage readings are obtained using the DC voltage sensor and subsequently displayed on the monitoring application. Moreover, the percentage of the accumulator can be computed using Equation (3).

$$Accu\ Percentage = \frac{DT - V_{min}}{V_{max} - V_{min}} \times 100\ % \tag{3}$$

In Equation (1), DT represents the accumulator voltage in the monitoring application. Vmin denotes the maximum limit of the accumulator voltage set at 14.9 volts, while Vmax represents the minimum limit set at 10.8 volts. Table 3 presents the results of the automatic switching test, showing the accumulator voltage readings from the voltmeter and monitoring system, the percentage difference between these readings, and the position of the power source (PLN or PLH). The voltage readings from the voltmeter ranged from 11.75 volts to 15 volts, while the monitoring system readings were slightly lower, ranging from 11.74 volts to 14.93 volts. The power source initially remained PLN for most of the readings, switching to PLH at higher voltages (around 15 volts) and back to PLN when the voltage was 11.75 volts. This behavior suggests a certain voltage threshold for switching between power sources. Overall, although the monitoring system was generally in sync with the voltmeter, the increasing difference at higher voltages indicated the need for calibration to improve accuracy. The system effectively manages power source transitions automatically.

Table 3. Automatic Switching Testing Results

| Accu Voltage | | Accu Percentage (%) | Power Source Position |
|------------------|-------------------|---------------------|-----------------------|
| Voltmeter (Volt) | Monitoring (Volt) | | |
| 11.75 | 11.74 | 25.36 | PLN |
| 12.00 | 11.97 | 28.53 | PLN |
| 12.50 | 12.38 | 38.53 | PLN |

| Accu Voltage | | Accu Percentage (%) | Power Source Position |
|------------------|-------------------|---------------------|-----------------------|
| Voltmeter (Volt) | Monitoring (Volt) | | |
| 13.00 | 12.81 | 49.02 | PLN |
| 13.50 | 13.28 | 60.49 | PLN |
| 14.00 | 13.80 | 73.17 | PLN |
| 14.50 | 14.36 | 86.83 | PLN |
| 15.00 | 15.03 | 100.00 | PLH |
| 14.50 | 14.39 | 87.56 | PLH |
| 14.00 | 13.81 | 73.41 | PLH |
| 13.50 | 13.29 | 60.73 | PLH |
| 13.00 | 12.88 | 50.73 | PLH |
| 12.50 | 12.37 | 38.29 | PLH |
| 12.00 | 11.96 | 28.29 | PLH |
| 11.75 | 11.73 | 22.93 | PLN |

Description: PLH: Source of Electricity from Hybrid Power Plant

PLN: Source of Electricity from PLN Electricity Network

4. Conclusion

In conclusion, the automatic switching system designed for hybrid power plants has proven to be effective in facilitating manual and automatic transitions between electrical energy sources. This includes selector switches or IoT applications, based on predefined accumulator voltage thresholds. The DC voltage sensor and ACS712 current sensor show small deviations in readings, with MAPE values of 2.959% and 3.577% for voltage and current, respectively. In addition, the DC voltage sensor showed reliable accuracy in the measurement of the accumulator voltage, with a MAPE value of 1% and a maximum error of 1.6%. Testing the PZEM-004T sensor on a 45-watt lamp load showed MAPE values of 0.604% and 8.625% for voltage and currents, with maximum errors of 1.602% and 15%, respectively. These results confirm the effectiveness of the designed system components in ensuring proper monitoring and switching operations in hybrid power plant configurations. The implication of research was enhancing the quality of maintenance scheduling and preventive interventions, preventing excessive accumulator draining to prolong the accumulator's service life, optimizes the use of renewable energy sources, reducing reliance on fossil fuels and promoting environmental sustainability.

References

- [1] C. D. P. Hertadi, M. Sulaiman, and P. G. P. Anwar, 'Kajian Industri Energi Terbarukan Tenaga Listrik di Indonesia Berdasarkan Arah Kebijakan dan Potensi Alam', *G-Tech J. Teknol. Terap.*, vol. 6, no. 2, pp. 276–283, 2022, doi: 10.33379/gtech.v6i2.1690.
- [2] H. Mamur, Ö. F. Dilmaç, J. Begum, and M. R. A. Bhuiyan, 'Thermoelectric generators act as renewable energy sources', *Clean. Mater.*, vol. 2, no. November, p. 100030, 2021, doi: 10.1016/j.clema.2021.100030.
- [3] P. Setianingsih and M. B. Husodo, 'Investasi Dan Analisis Kelayakan Ekonomi Pertambangan Terbuka Batubara Pt Gerbang Daya Mandiri Di Kalimantan Timur', *Sebatik*, vol. 26, no. 2, pp. 573–581, 2022, doi: 10.46984/sebatik.v26i2.2004.
- [4] T. A. Wahyu Sabubu, 'Pengaturan Pembangkit Listrik Tenaga Uap Batubara Di Indonesia Prespektif Hak Atas Lingkungan Yang Baik Dan Sehat', *J. Lex Renaiss.*, vol. 5, no. 1, pp. 72–90, 2020, doi: 10.20885/jlr.vol5.iss1.art5.
- [5] S. Muslim, K. Khotimah, and A. Azhiimah, 'Analisis Kritis Terhadap Perencanaan Pembangkit Listrik Tenaga Surya (Plts) Tipe Photovoltaic (Pv) Sebagai Energi Alternatif Masa Depan', *Rang Tek. J.*, vol. 3, no. 1, pp. 119–130, 2020, doi: https://doi.org/10.31869/rtj.v3i1.1638.
- [6] N. H. Jaenuri1, W. A. Nurtiyanto, and R. Subur, 'Analisis Efektifitas Penggunaan ATS dalam

- Meningkatkan Keandalan Pasokan Listrik dari PLTS Off-Grid’, *Kohesi J. Multidisiplin Saintek*, vol. 3, no. 5, pp. 100–111, 2024, doi: <https://doi.org/10.3785/kohesi.v3i5.3395>.
- [7] A. Asnil, K. Krismadinata, I. Husnaini, H. Hazman, and E. Astrid, ‘Real-Time Monitoring System Using IoT for Photovoltaic Parameters’, *TEM J.*, vol. 12, no. 3, pp. 1316–1322, 2023, doi: [10.18421/TEM123-11](https://doi.org/10.18421/TEM123-11).
- [8] F. Njoka, L. Thimo, and A. Agarwal, ‘Evaluation of IoT-based remote monitoring systems for stand-alone solar PV installations in Kenya’, *J. Reliab. Intell. Environ.*, vol. 9, no. 3, pp. 319–331, 2023, doi: [10.1007/s40860-022-00190-5](https://doi.org/10.1007/s40860-022-00190-5).
- [9] A. Triki-Lahiani, A. Bennani-Ben Abdelghani, and I. Slama-Belkhodja, ‘Fault detection and monitoring systems for photovoltaic installations: A review’, *Renew. Sustain. Energy Rev.*, vol. 82, no. March, pp. 2680–2692, 2018, doi: [10.1016/j.rser.2017.09.101](https://doi.org/10.1016/j.rser.2017.09.101).
- [10] M. Gopal, T. Chandra Prakash, N. Venkata Ramakrishna, and B. P. Yadav, ‘IoT Based Solar Power Monitoring System’, *IOP Conf. Ser. Mater. Sci. Eng.*, vol. 981, no. 3, pp. 1–8, 2020, doi: [10.1088/1757-899X/981/3/032037](https://doi.org/10.1088/1757-899X/981/3/032037).
- [11] S. Sarswat, I. Yadav, and S. K. Maurya, ‘Real Time Monitoring of Solar PV Parameter Using IoT’, *Int. J. Innov. Technol. Explor. Eng.*, vol. 9, no. 1S, pp. 267–271, 2019, doi: [10.35940/ijitee.a1054.1191s19](https://doi.org/10.35940/ijitee.a1054.1191s19).
- [12] T. Sutikno, H. S. Purnama, A. Pamungkas, A. Fadlil, I. M. Alsofyani, and M. H. Jopri, ‘Internet of things-based photovoltaics parameter monitoring system using NodeMCU ESP8266’, *Int. J. Electr. Comput. Eng.*, vol. 11, no. 6, pp. 5578–5587, 2021, doi: [10.11591/ijece.v11i6.pp5578-5587](https://doi.org/10.11591/ijece.v11i6.pp5578-5587).
- [13] A. Readyansyah, S. Haryudo, A. Achmad, and N. Kholis, ‘Perancangan Pembangkit Listrik Hybrid (Solar Cell – Thermoelectric Generator (TEG)) Berbasis Internet of Things (IoT)’, *J. Tek. Elektro*, vol. 11, no. 03, pp. 454–464, 2022, doi: <https://doi.org/10.26740/jte.v11n3.p454-462>.
- [14] I. F. Pamungkas, U. T. Kartini, T. Wrahatnolo, and Joko, ‘Sistem Monitoring Daya Listrik Photovoltaic Berbasis Internet of Things (IoT)’, *J. Tek. Elektro*, vol. 11, no. 2, pp. 236–245, 2022, doi: <https://doi.org/10.26740/jte.v11n2.p236-245>.
- [15] I. Inayah, N. Hayati, A. Nurcholis, A. Dimiyati, and M. G. Prasetya, ‘Realtime Monitoring System of Solar Panel Performance Based on Internet of Things Using Blynk Application’, *Elinvo (Electronics, Informatics, Vocat. Educ.)*, vol. 7, no. 2, pp. 135–143, 2023, doi: [10.21831/elinvo.v7i2.53365](https://doi.org/10.21831/elinvo.v7i2.53365).
- [16] M. Rajvikram and G. Sivasankar, ‘Experimental study conducted for the identification of best heat absorption and dissipation methodology in solar photovoltaic panel’, *Sol. Energy*, vol. 193, no. March, pp. 283–292, 2019, doi: [10.1016/j.solener.2019.09.053](https://doi.org/10.1016/j.solener.2019.09.053).
- [17] A. Antony, Y. D. Wang, and A. P. Roskilly, ‘A detailed optimisation of solar photovoltaic/thermal systems and its application.’, *Energy Procedia*, vol. 158, no. 2018, pp. 1141–1148, 2019, doi: [10.1016/j.egypro.2019.01.295](https://doi.org/10.1016/j.egypro.2019.01.295).
- [18] T. Ratnasari and A. Senen, ‘Perancangan prototipe alat ukur arus listrik Ac dan Dc berbasis mikrokontroler arduino dengan sensor arus Acs-712 30 ampere’, *J. Sutet*, vol. 7, no. 2, pp. 28–33, 2017, doi: <https://doi.org/10.33322/sutet.v8i1.713>.
- [19] P. L. dos Santos, T. P. A. Perdicoulis, P. A. Salgado, and J. C. Azevedo, ‘Kalman filter for noise reduction of Li-Ion cell discharge current’, *IFAC-PapersOnLine*, vol. 56, no. 2, pp. 9582–9587, 2023, doi: [10.1016/j.ifacol.2023.10.261](https://doi.org/10.1016/j.ifacol.2023.10.261).
- [20] D. Li, Y. Wang, J. Wang, C. Wang, and Y. Duan, ‘Recent advances in sensor fault diagnosis: A review’, *Sensors Actuators, A Phys.*, vol. 309, p. 111990, 2020, doi: [10.1016/j.sna.2020.111990](https://doi.org/10.1016/j.sna.2020.111990).